Laurus nobilis green inhibitor for patinated bronze protection in sulfate media

Aymen Chaabani[a,b], Safa Aouadi[a,b], Mhamed Ben Messaouda[c], Adel Moadhen[d], Adel Madani[e] ,Nizar Bellakhal[f], Nébil Souissi[a*]

[a]*University of Tunis El Manar, Institut Préparatoire aux Etudes d'Ingénieurs d'ElManar, Campus Universitaire Farhat Hached d'ElManar, BP 244 El Manar II 2092, Tunisia.*
[b]*University of Carthage, Faculté des Sciences de Bizerte 7021 Jarzouna- Tunisia.*
[c]*University of Carthage, Institut Préparatoire aux Etudes Scientifiques et Techniques de la Marsa, BP 51 la Marsa 2070, Tunisia.*
[d]*University of Tunis El Manar, Unité de Recherche « Spectroscopie Raman », Faculté des Sciences de Tunis, Campus universitaire Farhat Hached d'El Manar, 2092 El Manar, Tunisia.*
[e]*Umm Al Qura University Applied Science College, Department of Physics, Mekkah, KSA.*
[f]*University of Carthage, Institut National des Sciences Appliquées et de Technologie (INSAT), Unité de Recherche « CENAD » 1080 Tunis, Cedex Tunisia.*

(Received: 13 September 2016, accepted 17 November 2016)

Abstract: The inhibiting effect of *Laurus nobilis* extract on the corrosion behaviour of patinated bronze was evaluated by means of potentiodynamic polarization, statistical experimental design, Raman spectroscopy and quantum chemical calculations. The patina layer was electrodeposited at the Cu10Sn bronze alloy in aqueous chloride electrolyte under anodic conditions. Electrochemical and Raman characterizations showed the presence of various tin oxides and crystallized as well as porous cuprite in the chloride patina layer. The statistical experimental design was investigated to model the *Laurus nobilis* inhibition of the patinated bronze in sulfate electrolyte. The plant extract was found to act as mixed type inhibitor. The relatively low protection efficiency was related to the synergetic effect between the experimental parameters. Quantum chemical calculations were performed with the DFT method at the B3LYP/3-21G basis set. The results revealed that the major molecule inhibitor could interact preferentially with tin oxide.

Keywords: Cu10Sn alloy, patinated bronze, green inhibitor, experimental design, DFT.

INTRODUCTION

Copper tin alloys undergo significant corrosion process during their exposure in aggressive media. Hence, a thin patina layer could be developed at the bulk material surface. Therefore, the protection of bronze objects becomes of great importance.

The use of corrosion inhibitors is one of the most protecting methods for bronze preservation. Numerous studies studied organic inhibitors which revealed efficient protection for bronze materials [1-5]. However, these compounds are toxic and present negative impact on the environment. In the last decades, several research papers focused on the use of non-toxic and ecofriendly inhibitors for corrosion control [6-12]. Nevertheless, few works investigated green inhibitors for bronze preservation. In fact, Hammouch *et al* [13] tested the inhibiting effect of *Opuntiaficus indica* seed extract for pre-patinated bronze. The electrochemical results revealed a significant improvement of bronze inhibition with the extract addition. In our previous work, we evaluated the *Juniperus communis* alcoholic extract for Cu10Sn bronze alloy inhibition in chloride medium. The inhibition efficiency reached 62%indicating that such extract could be promising for bronze preservation [14].

The inhibition efficiency of the green extracts may depend on the experimental conditions. Indeed, the chemometric approach is the best method to study complex corrosion protection process with reduced experiments. Current research efforts focus on the

* Corresponding author, e-mail address : nebil.souissi@utm.tn

use of the statistical experimental design to study corrosion and corrosion prevention of metals [15-21]. Recently, we used a Plackett-Burman experimental design to model the experimental conditions for PANI bronze corrosion protection in chloride medium [22]. The screening study allowed us identifying the optimum electrodeposition conditions which generated important protection efficiency to the Cu10Sn bronze alloy.

The aim of the present work was to investigate the effect of *Laurus nobilis* extract on the corrosion behavior of chloride patinated bronze in neutral aqueous sulfate medium using potentiodynamic measurements. The full factorial experimental design was chosen to study the effect of immersion time in the extract and the plant mass on the electrochemical responses. Raman spectroscopy characterization and quantum chemical calculations were carried out in order to elucidate the interaction between the chloride patina layer and the inhibitor molecules.

EXPERIMENTAL

The *Laurus nobilis* extract was prepared using maceration method: The plant leaves were soaked in water (v = 150 mL) for 24 hours. The obtained solution was then filtered and used without further treatment.

The working electrode was elaborated from a synthetic Cu10Sn bronze alloy through a procedure described above [23]. The electrochemical experiments were carried out in a classical three-electrode cell with a platinum wire as counter electrode and a calomel electrode in saturated KCl solution (SCE) as reference. The bronze was used as working electrode with an active area equal to $0.33cm^2$. The material was embedded in a chemically inert resin and mechanically polished up to 2500 SiC grade before use. The experiments were conducted on a PGSTAT 30 potentiostat-galvanostat. GPES software was used for instrumentation control and data treatments.

The chloride patina layer was electrochemically prepared at the Cu10Sn bronze alloy. The substrate was immersed in a chloride electrolyte (0.1M NaCl solution) at open circuit potential (E_{ocp}) for one hour. The electrode was then polarized from $E_{ocp}$to 1V/SCE at a scan rate of $1mVs^{-1}$.

The corrosion test was performed in $1g.L^{-1}$ sulfate electrolyte. The potentiodynamic measurements started at E_{ocp} reached after five minutes of immersion in the corrosive electrolyte. The anodic domain ranged from E_{ocp} to 0.5V/SCE whereas the cathodic interval was from E_{ocp} to -2V/SCE. The scan rate was fixed at$1mVs^{-1}$.

The Raman spectra were recorded at room temperature with a T64000, Jobin-Yvon spectrometer.

Quantum chemical calculations were performed using DFT method at the B3LYP/3-21G level set, all the calculations were carried out with Gaussian 03 [24].

RESULTS AND DISCUSSION

1. Electrochemical characterization

The Cu10Sn bronze alloy was immersed in aqueous chloride electrolyte for one hour. The electrode was polarized from E_{ocp} to 1V/SCE at a scan rate of $1mVs^{-1}$ and the result was given in Fig.1.

The obtained anodic polarization curve was consistent with those found in the literature for archaeological and modern bronze materials immersed in aqueous chloride electrolyte [25-27]. In fact, three anodic domains were evidenced. The first interval characterized by a current density increase was attributed to the anodic Tafel part. It was followed by an anodic current peak at 0.157V/ SCE with a maximum at 1.8 $mAcm^{-2}$corresponding to the simultaneous oxidation of tin and copper species [25, 26].

Finally, the current density decreased and a current plateau was evidenced. It could reflect the

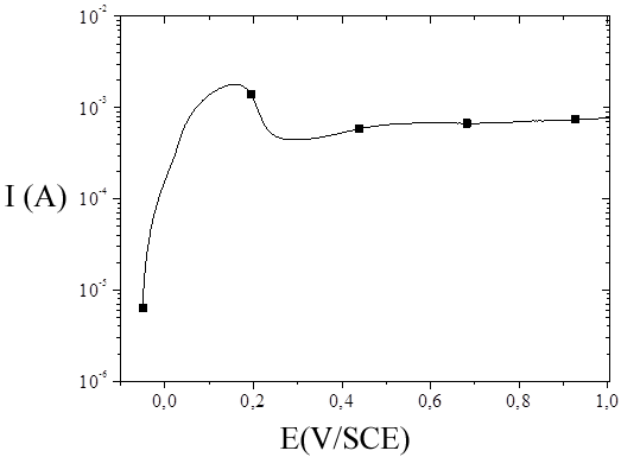

Fig.1: The anodic polarization curve of the Cu10Sn bronze alloy immersed for one hour in 0.1M NaCl solution, at a scan rate fixed at $1mVs^{-1}$.

formation of patina layer containing cuprous chloride and tinhydroxychloride [25,26].

The electrochemical behaviour of the chloride patinated bronze was then studied in 1g.L^{-1} Na_2SO_4 solution. The polarization curves of the patinated bronze compared to the bare one were plotted after five minutes of immersion in the sulfate medium at a scan rate of 1mVs^{-1}. Fig.2 presents the obtained I-E curves.

For the anodic scan, the polarization curve of the blank showed three successive regions (Fig.2a). The first part at the vicinity of E_{ocp} was attributed to the anodic Tafel interval. In the second region, the current density decreased and a pseudo-passive layer occurred reflecting the growth of a passive film at the bronze surface. Finally, the current density increased which indicated the substrate dissolution through the formed layer. In the presence of the patina layer, the bronze substrate behaved differently as a single dissolution ramp was evidenced in the whole anodic domain.

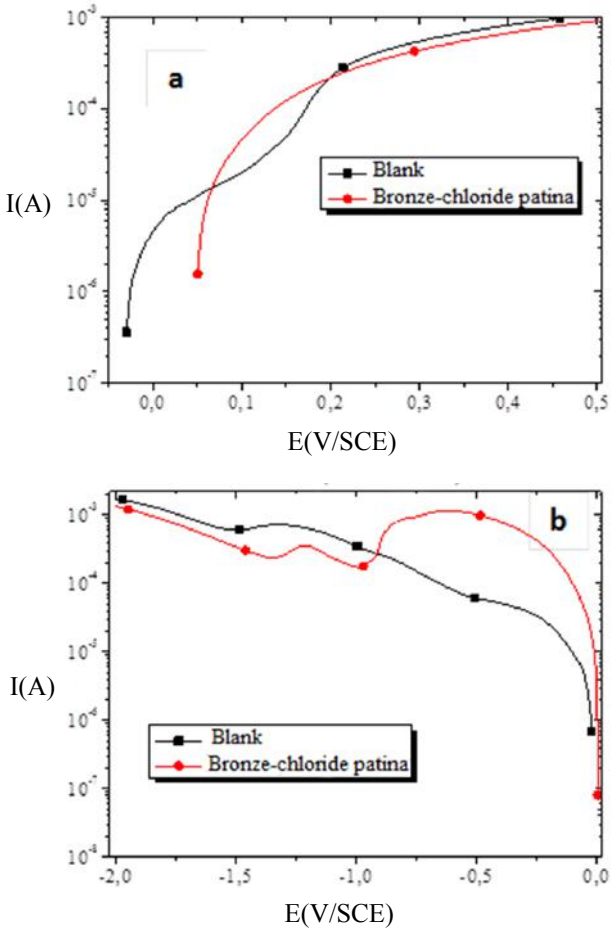

Fig.2: The I-E curves of the bronze electrode immersed for five minutes in 1g.L^{-1} Na_2SO_4 solution without and with the patina layer (a) anodic range, (b) cathodic range, the scan rate fixed at 1mVs^{-1}.

The cathodic polarization curves for the blank and patinated bronze could be divided to three intervals (Fig.2b). Firstly, the cathodic Tafel part occurred at the vicinity of E_{ocp}. Then, one can note the appearance of current peaks at -0.3V/SCE and -0.6V/SCE for the blank and the patinated bronze, respectively, which could correspond to copper species reduction. The second peak appearing at lower potentials was linked to the reduction of tin compounds. In the last region, the current density markedly increased indicating the solvent reduction.

From the Tafel domain, the extrapolation of linear line to corrosion potential (E_{corr}) gives a straight line, the slope gives both β_a and β_c, and the intercept gives the corrosion current (I_{corr}). Furthermore, Tafel slopes extrapolations were used to determine the proportionality factor (B) and the polarization resistance (R_p) according to the following Stern-Geary equations [32]:

$$B = \frac{\beta_a \beta_c}{2.3(\beta_a + \beta_c)} \quad (1)$$

$$Rp = \frac{\beta_a \beta_c}{2.3(\beta_a + \beta_c)} \frac{1}{Icorr} \quad (2)$$

Table I summarized the electrochemical parameters for the bare and patinated bronze.

After five minutes of immersion in the sulfate electrolyte, it was found that the corrosion potential shifted to the anodic region in the presence of the patina layer. Such a behaviour could reflect the substrate passivation. Furthermore, the anodic Tafel slope was 0.191V/dec for the interface blank/Na_2SO_4. It was reduced when the chloride patina was deposited at the bronze surface indicating the modification of the corrosion process. As for the cathodic Tafel slope, it was found that the interface blank /Na_2SO_4 generated the highest value. The difference between βc could be related to different electron exchange of the cathodic reaction.

The proportionality factor values remained in the range of B encountered for copper based materials [28]. It is important to note that the corrosion current density increased in the presence of the patina layer. Such a result could be related to the porous structure of the chloride patina which

Table I: Electrochemical parameters of the bronze substrate without and with the patina deposition

	E_{corr} (V/SCE)	β_a (V/dec)	β_c (V/dec)	B (mV)	I_{corr} (μAcm^{-2})	R_p ($\Omega\ cm^{-2}$)
bare	-0.025	0.191	-0.019	7.5	4.3	1747.3
patina	0.028	0.094	-0.145	24.8	15.9	1559.5

accelerated the metal dissolution in the sulfate electrolyte. Therefore the highest polarization resistance value was found for the blank.
From the previous results, it could be concluded that chloride patinated bronze exhibited particular electrochemical behaviour in the sulfate electrolyte. This could be linked to the complex structure of the patina layer containing poorly crystallized copper species and tin hydroxychloride compounds.

2. Statistical experimental design study

The statistical experimental design approach was performed in order to model the experimental conditions of the patinated bronze inhibition in sulfate electrolyte. A full factorial design was chosen in order to evaluate the influence of n variables on the experimental responses. Therefore I^n experiments would be conducted [15].

Table II: Experimental field

Level	U_1 plant mass (g)	U_2 immersion time in the extract(min)
-1	100	30
+1	200	180

Table III: Experimental design - Experimental matrix

	Experimental design		Experimental matrix	
Experiment	U_1	U_2	X_1	X_2
1	100	30	-1	-1
2	200	30	+1	-1
3	100	180	-1	+1
4	200	180	+1	+1

After a preliminary investigation two experimental factors were considered:
U_1: first factor representing the plant mass,
U_2: second factor representing the immersion time in the extract,
The first factor was chosen to simulate the active species concentration of the extract. As for the second one, it was selected with the aim of modeling the physical phenomena related to the adsorption and / or diffusion of the active species through the chloride patina layer.
These two variables were studied at two levels: -1 for the low level and +1 for the high level. Table II gathered the experimental field.
The experimental design consisted of four experiments. The experimental design and the corresponding experimental matrix were presented in Table III.
The experimental responses considered in this study were the electrochemical parameters obtained from the Tafel extrapolation (E_{corr}, β_a, β_c, I_{corr}, B, Rp), the cathodic copper consumed charge (Q_{Cu}), the cathodic tin consumed charge (Q_{Sn}) and the inhibition efficiency estimated from the following equation [14]:

$$\%\ IE = \frac{Icorr(B) - Icorr(B+LN)}{Icorr(B)} \qquad (3)$$

where:
- I_{corr} (B) is the corrosion current density of the blank,
- I_{corr} (B+LN) is the corrosion current density in the presence of the Laurusnobilis extract.

A linear mathematical model was employed where the experimental responses could be represented by the following equation:

$$Y_i = b_0 + b_1X_1 + b_2X_2 + b_{12}X_1X_2 \qquad (4)$$

where:
- Y_i is the response,

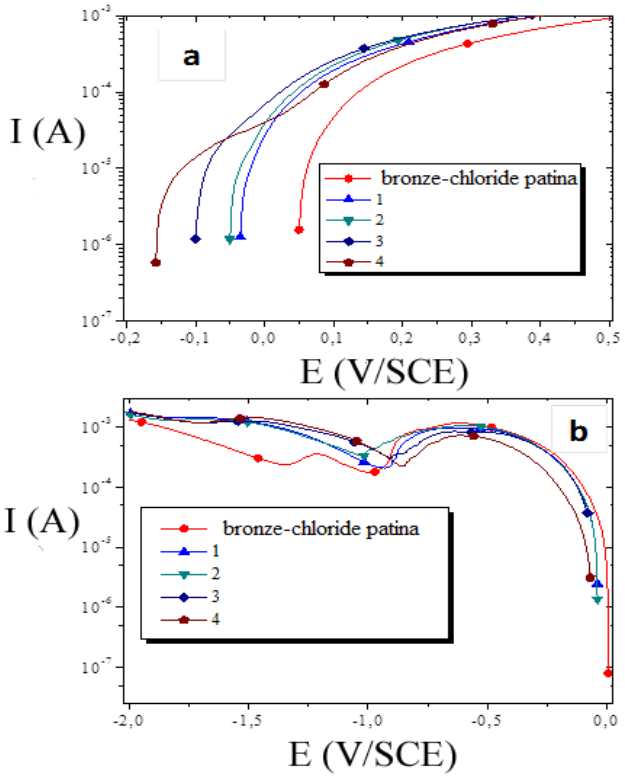

Fig.3: Polarization curves of the patinated bronze in the presence of the extract according to the experimental design (a) anodic range, (b) cathodic range. Scan rate fixed at $1mVs^{-1}$.

- X_i is the coded variable relative to natural variable U_i, which obtained as detailed elsewhere [15],
- b_0 is the intercept,
- bi represents the coefficient of the main effects of the factor i,
- bij represents the coefficient of the interaction between the two factors i and j.

The chloride patinated bronze treated with the inhibitor according to the experimental conditions described above was submitted in $1g.L^{-1}$ Na_2SO_4 electrolyte for five minutes. The electrode was then polarized from E_{ocp} to 0.5V/SCE (anodic scan) and from E_{ocp} to -2V/SCE (cathodic scan) at a scan rate of $1mVs^{-1}$, the results were given in Fig.3.

It was found that the electrochemical behaviour of the patinated bronze was affected by the inhibitor addition. The electrochemical parameters extracted from the Tafel region were listed in Table IV. It was found that both the anodic and cathodic Tafel slopes were modified by the extract addition. Hence, we concluded that the *Laurus nobilis* extract acted as a mixed type inhibitor.

The responses were analyzed by regression analysis according to the proposed mathematical model. Furthermore, to explain the responses change and to evaluate the weight of the different coefficients of the model Pareto analysis was performed [29].

The percentage effect Pi of each term i, was estimated through the relationship:

$$Pi = 100\left(\frac{bi^2}{\sum_i bi^2}\right) \quad (5)$$

Fig.4 depicts the analysis of the different experimental responses.

For the different electrochemical parameters, it could be mentioned that the positive sign of the model coefficient reflected positive evolution of the response and the negative values indicated negative variation of the response (Fig.4a). Furthermore analysis of the Pareto charts showed that (Fig.4b-c):

- b_2 could explain about 92% of the corrosion

Table IV: Experimental responses extracted from the polarization curves

	E_{corr} (V/SCE)	β_a (V/dec)	β_c (V/dec)	I_{corr} (μAcm^{-2})	B (mV)	R_p ($\Omega\ cm^{-2}$)	Q_{Cu} ($mCcm^{-2}$)	Q_{Sn} ($mCcm^{-2}$)	IE (%)
blank	0.028	0.094	-0.145	15.9	24.8	1559.5	0.78	0.44	-
1	-0.037	0.091	-0.086	13	19.2	1478.8	0.52	2.36	-5.5
2	-0.045	0.139	-0.098	19.4	25.0	1288.1	0.60	2.29	-21.1
3	-0.089	0.271	-0.079	47.5	26.6	559.9	0.46	1.79	-178
4	-0.114	0.234	-0.070	9.4	23.4	2492.2	0.36	1.98	37.4

E_{corr}

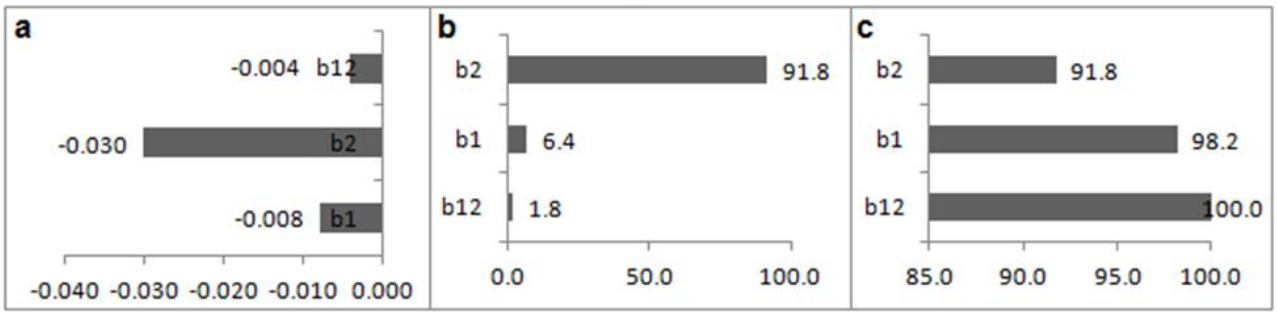

β_a

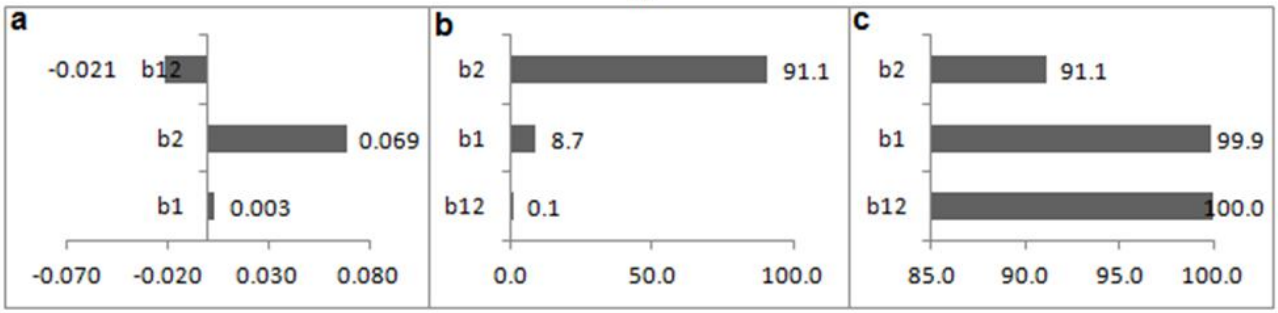

β_c

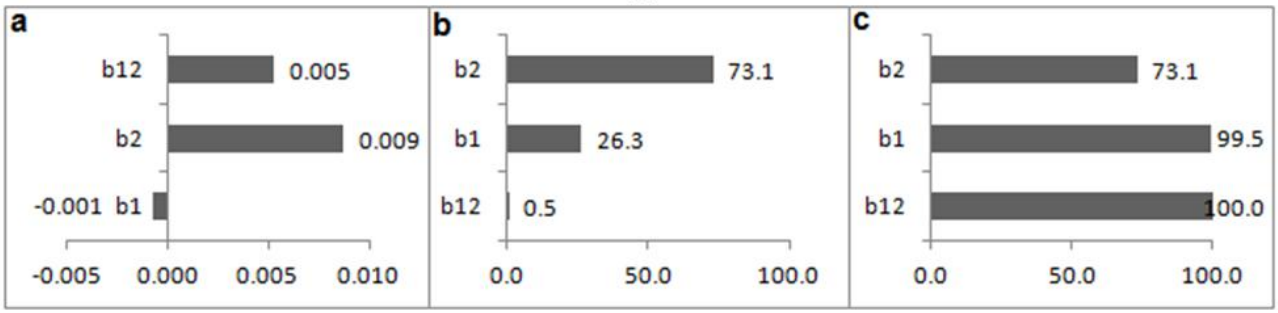

B

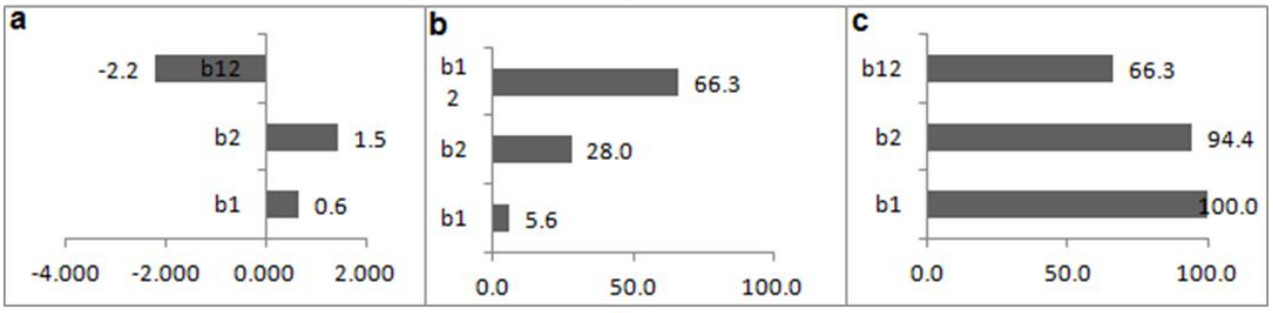

I_{corr}

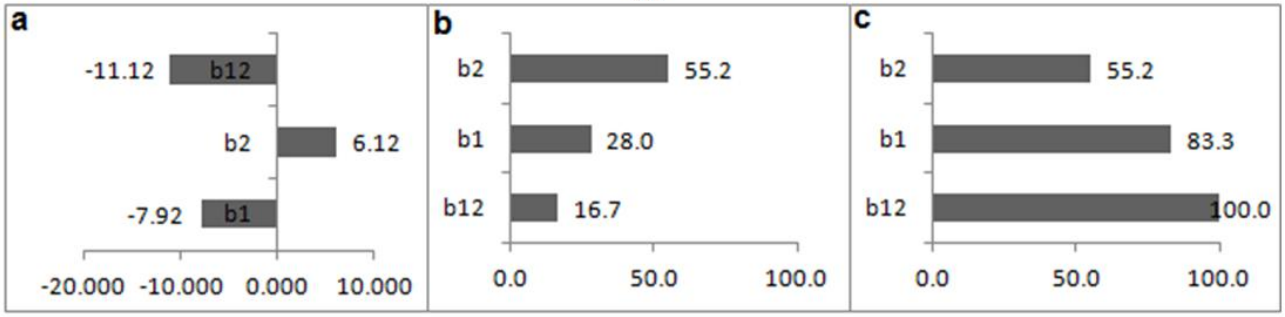

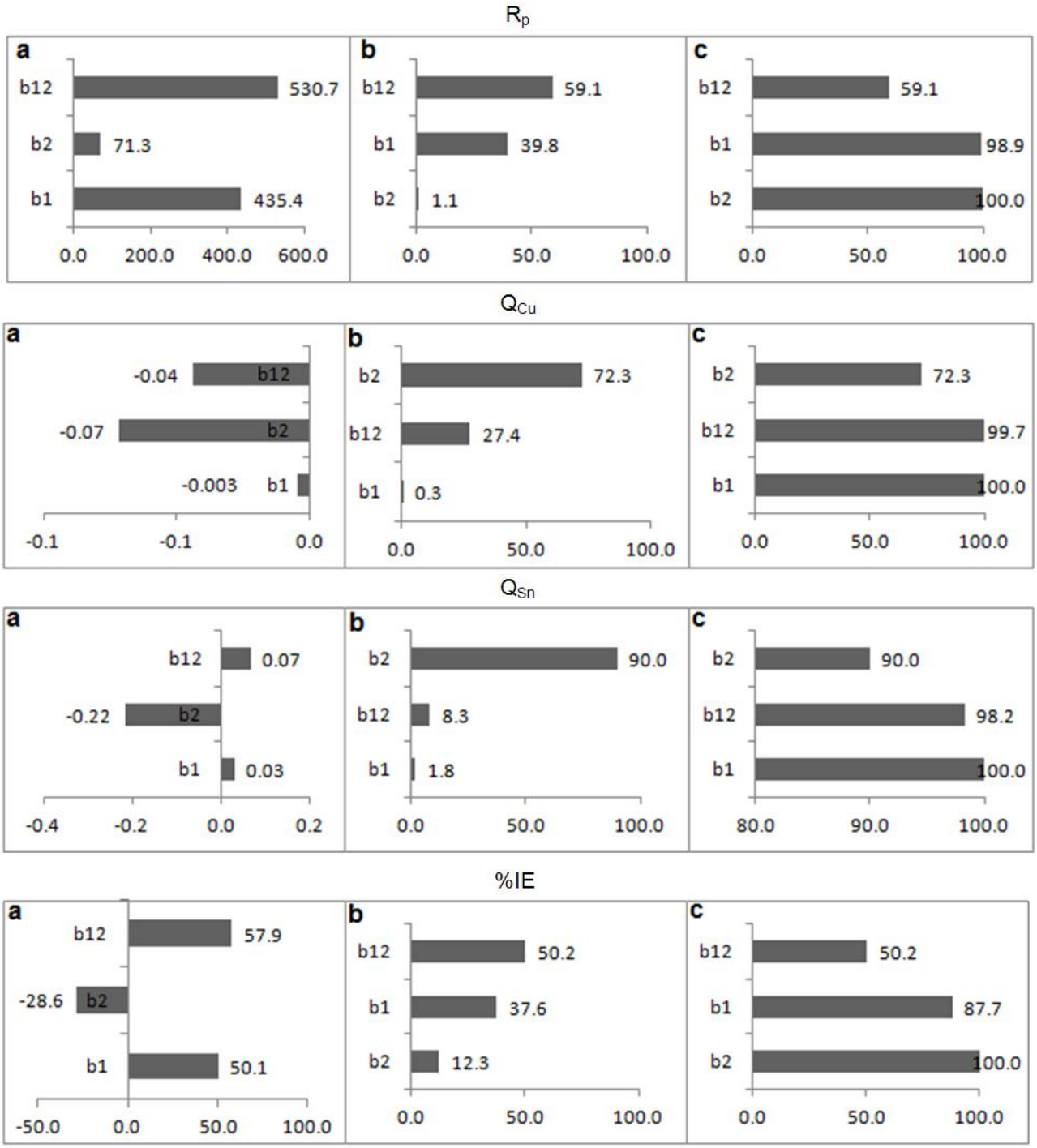

Fig.4: (a) The estimated model coefficients, (b) Pareto charts and (c) cumulative Pareto charts for the different electrochemical responses

potential variation. The main effect was related to the immersion time in the extract (P_2 = 92%).

- The factor b_2 represented about 91% of the anodic Tafel slope variation. So the most influent parameter was the immersion time in the extract as P_2 = 91%.
- b_1 and b_2 were the significant factors for the cathodic Tafel slope variation. The main effect was attributed to the immersion time in the extract since P_2= 73%.
- b_2 and b_{12} allowed the explanation of 95% of the proportionality factor variation. The most

important effect was linked to the interaction between the factors (P_{12}= 66%).

- b_1 and b_2 were the influent factors for the corrosion current density variation. The immersion time in the extract was the most important (P_2 = 55.2%).
- b_1 and b_{12} could contribute about 99% of the polarization resistance. The interaction between the factors was the most significant (P_{12}= 59.1%).
- 99% of the copper consumed charge variation was due to b_2 and b_{12}. The immersion time in the extract was the most significant as (P_2= 72.3%)
- b_2 was the most influent effect for tin charge consumed variation as P_2 was about 90%.
- b_1 and b_{12} presented about 88% of the inhibition efficiency variation. The interaction between experimental parameters was the most influent (P_{12}= 50.2%).

From the previous observations, we concluded that the immersion time in the extract was the most influent factor for E_{corr}, β_a, β_c, I_{corr}, Q_{Cu} and Q_{Sn} variation. Therefore, the interfacial phenomena related to the adsorption and/or diffusion were the most predominant for these electrochemical responses. On the other hand, we found that the interaction between the immersion time in the extract and the plant mass was the most important for B, R_p and %IE. So the synergistic effect between the experimental parameters was dominant for the considered responses.

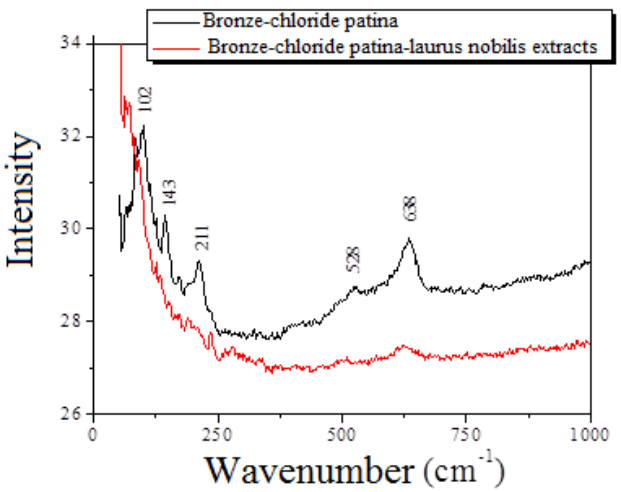

Fig.5: Raman spectra of patinated bronze without and with the extract addition

3. Raman spectroscopy characterization

The chloride patina layer was initially formed at the bronze surface without and with the extract addition. The covered electrode covered was then characterized by Raman spectroscopy analysis. Fig. 5 shows the Raman spectra for the patinated bronze and in the presence of extract recorded in the spectral range 100-1000 cm^{-1}.

For the chloride patinated bronze, five main Raman bands were evidenced. In the low spectral range, the first band located at 102 $cm^{-1}$was assigned toSnO_2nanocrystals with a size within 8-10nm [30]. The second band at 143cm^{-1} was related to neither SnO nor SnO_2. According to literature results, when using X-ray diffraction technique, it was reported that this band to attributed this band to SnO_x sub-oxide ($1<x<2$) [30]. The band occurring at 638cm^{-1} could be ascribed to the cassiterite SnO_2 [30].

Moreover, the bands located at 211cm^{-1} et 528cm^{-1} could be related to the cuprite Cu_2O : the first band could correspond to crystallized molecules, while the second one was related to porous species [30].

It was observed that the extract addition provided a change on bronze interfacial behaviour as Raman spectrum showed a modification (Fig.5). The bands intensity related to tin compounds was markedly reduced. Therefore, it could be concluded that the *Laurus nobilis* extract could interact preferentially with tin species.

4. Quantum Chemical calculations

In order to elucidate the interaction between the inhibitor molecules and the chloride patina layer grown at the bronze surface the quantum chemical investigation was conducted. In fact, a previous research on the *Laurus nobilis* plant structure showed that α-terpinene (TERP) was the major molecule (Fig.6) [31].

The quantum calculations were made using DFT method at the B3LYP/3-21G basis set. The

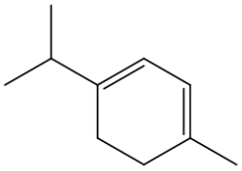

α-terpinene

4-methyl-1-(1-methylethyl)-1,3-cyclohexadiene

Fig.6: α-terpinene structure

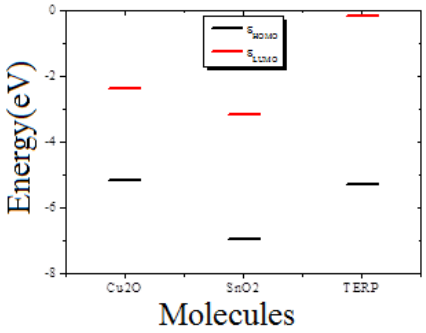

Fig.7: Energy diagram for cuprite (Cu_2O), cassiterite (SnO_2) and α-terpinene.

quantum chemical parameters E_{HOMO} and E_{LUMO} which are characteristic to electron donating and electron accepting were determined for Cu_2O, SnO_2 and α-terpinene and the results were summarized in Fig.7.

It was evidenced that $\varepsilon_{LUMO}(SnO_2) < \varepsilon_{LUMO}$ (Cu_2O) reflecting the ability of SnO_2 to accept electrons. Furthermore, the energy gap Δε (Δε = ε_{LUMO} (oxide) - ε_{HOMO}(TERP)) was estimated for the different oxides. It was found that $\Delta\varepsilon(SnO_2)$(2.111 eV) was lower than $\Delta\varepsilon(Cu_2O)$ (2.906 eV). Such a result revealed the preferential electronic reactivity between α-Terpinene and tin oxide.

CONCLUSION

In the present work, electrochemical measurements, the chemometric approach, Raman spectroscopy analysis and quantum calculations were conducted to study the inhibiting effect of *Laurus nobilis* extract on patinated Cu10Sn bronze alloy in sulfate electrolyte. The chloride patina was electrochemically synthesized at the bronze substrate under anodic conditions. Raman spectroscopy characterization of the chloride patina showed the presence of various tin oxides as well as crystallized and porous cuprous. A full factorial design was used to model the experimental conditions of the patinated bronze inhibition in sulfate electrolyte. the statistical results showed that the immersion time in the extract was the most significant factor for E_{corr}, β_a, β_c, I_{corr}, Q_{Cu} and Q_{Sn} variation, while the inter-action between the experimental parameters was the most influent for the responses B, R_p and %IE. Analysis of the electrochemical responses allowed us concluding that the plant extract was classified as a mixed type inhibitor. The low inhibition efficiency was related to the synergetic effect between the experimental parameters. Quantum chemical calculations and Raman analysis revealed that the major molecule inhibitor acted preferentially with tin oxide.

REFERENCES

[1] L. Muresan, S. Varvara, E. Stupnišek-Lisac, H. Otmačić, K. Marušić, S. Horvat-Kurbegović, L. Robbiola, K. Rahmouni, H. Takenouti, Electrochim. Acta. **2007**, 52, 7770-7779.
[2] K. Rahmouni, N. Hajjaji, M. Keddam, A. Srhiri, H. Takenouti, Electrochim. Acta. **2007**, 52, 7519-7528.
[3] A. Dermaj, N. Hajjaji, S. Joiret, K. Rahmouni, A. Srhiri, H. Takenouti, V. Vivier, Electrochim. Acta. **2007**, 52, 4654-4662.
[4] K. Rahmouni, H. Takenouti, N. Hajjaji, A. Srhiri, L. Robbiola, Electrochim. Acta. **2009**, 54 , 5206-5215.
[5] S. Varvara, L.M. Muresan, K. Rahmouni, H. Takenouti, Corros. Sci. **2008**, 50, 2596-2604.
[6] P.B. Raja, M.G. Sethuraman, Mater. Lett **2008**, 62 , 113-116.
[7] B.E.A. Rani, B.B.J. Basu, International Journal of Corrosion. **2012**, 1-15.
[8] M. Abdullah Dar, Ind. Lub. Tribol.**2011**, 63, 227-233.
[9] D. Kesavan, M. Gopiraman, N. Sulochana, Chem. Sci. Rev. Lett. **2012**, 1,1-8.
[10] F. Suedile, F. Robert, C. Roos, M. Lebrini, Electrochim.Acta.**2014**, 133, 631-638.
[11] A. Khadraoui, A. Khelifa, H. Hamitouche, R. Mehdaoui, Res. Chem. Intermed.**2013**, 40 , 961-972.
[12] M.A. Deyab, J. Taiwan. Inst. Chem.Eng. **2016**, 58 , 536-541.
[13] H. Hammouch, A. Dermaj, M. Goursa, N. Hajjaji, A. Srrhiri, Proceedings of the international conference on conservation strategies for saving indoor metallic collections with a stallite meeting on legal issues inn the conservation of cultural heritage. Cairo TEI of Athens. **2007**, 149-155.
[14] R. Ben Channouf, N. Souissi, N. Bellakhal, J. Mater. Sci. Chem. Eng. **2015**, 3, 21.
[15] N. Souissi, E. Triki, Corros. Sci. **2008**, 50, 231-241.
[16] G. Luciano, P. Traverso, P. Letardi, Corros. Sci. **2010**, 52, 2750-2757.
[17] M. Hajeeh, Mater. Des. **2003**, 24, 509-518.
[18] E.C. Rios, A.M. Zimer, P.C.D. Mendes, M.B.J. Freitas, E.V.R. de Castro, L.H. Mascaro, E.C. Pereira, Fuel. **2015**, 150, 325-333.
[19] I. Forsal, M.E. Touhami, B. Mernari, J.E. Hajri, M.F. Baba, Port. Electrochim. Acta. **2010**, 28, 203-212.
[20] D. Mondel, S. Das, B. Prasad, Wear. **1998**, 217, 1-6.

[21] F.J.R. de Oliveira, D.C.B. Lago, L.F. Senna, L.R.M. de Miranda, E. D'Elia, Mater. Chem. Phys.**2009**, 115 ,761-770.
[22] S. Aouadi, N. Souissi. Surf. Interface. Anal. **2016**, doi 10.1002.sia.6050.
[23] E. Sidot, N. Souissi, L. Bousselmi, E. Triki, L. Robbiola, Corros. Sci. **2006**, 48, 2241-2257.
[24] M.J. Frisch, G. W. Trucks, H. B. Schlegel , G. E. Scuseria, M. A. Robb, J. R. Cheeseman, V. G. Zakrzewski, J. A. Montgomery, J. R. Stratmann, R. E. Burant, J. C. Dapprich, S. Millam, J. M. Daniels, A.D. Kudin, K. N. Strain, M. C. Farkas, O. Tomasi, J. Barone,V. Cossi, M. Cammi, R. Mennucci, B. Pomelli, C. Adamo, C. Clifford, S. Ochterski, J. Peterson, G. A. Ayala, P. Y. Cui, Q. Morokuma, K. Malick, D. K . Rabuck, A. D. Raghavachari, K.Foresman, J. B. Cioslowski, J. Ortiz, J. V. Baboul, A. G. Stefanov, B. B. Liu,G. Liashenko,A. Piskorz,P. Komaromi,I. Gomperts, R. Martin, R. L. Fox, D. J. Keith,T. Al-Laham,M.A. Peng, C. Y. Nanayakkara, A. Gonzalez, C. Challacombe, M. Gill, P. M. W. Johnson, B. Chen, W. Wong, M.W. Andres, J. L. Gonzalez, J. A. Pople, Gaussian 03, Revision C01, Gaussian, Inc, Walling ford, CT, **2004**.
[25] N. Souissi, E. Sidot, L. Bousselmi, E. Triki, L. Robbiola, Corros. Sci. **2007**, 49,3333-3347.
[26] L. Robbiola, T.T.M. Tran, P. Dubot, O. Majerus, K. Rahmouni, Corros.Sci. **2008**, 50, 2205-2215.
[27] N. Souissi, L. Bousselmi, S. Khosrof, E. Triki, Mater. Corros. **2004**, 55, 284-292.
[28] G. Kear, B.D. Barker, F.C. Walsh, Corros. Sci. **2004**, 46 , 109-135.
[29] P.D. Haaland, New York, **1989**.
[30] F. Ospitali, C. Chiavari, C. Martini, E. Bernardi, F. Passarini, L. Robbiola, J . Raman Spectrosc. **2012**, 43 , 1596-1603.
[31] I. Kahouli, Effet antioxydant d'extraits de plantes (*Laurus nobilis* L., *Rosmarinus officinalis*, *Origanum majorana*, *Oléa Europea* L.) dans l'huile de canola chauffée, Université Laval, **2010**.
[32] L. Stern, A. L. Geary, J. Electrochem. Soc. **1957**, 104, 56.